

Epitaxial growth of Fe-Si compounds on the silicon (111) face

Le Thanh Vinh, J. Chevrier, and J. Derrien

*Centre de Recherche sur les Mécanismes de la Croissance Cristalline, Campus de Luminy,
case 913, 13288 Marseille CEDEX 09, France*

(Received 24 February 1992)

In a molecular-beam-epitaxy (MBE) chamber, epitaxial growth of all the silicides existing in the low-temperature portion of the iron-silicon phase diagram [e.g., bcc Fe (+Si), FeSi, and the semiconducting silicide β -FeSi₂] was achieved on the (111) face of silicon by deposition of pure iron onto a heated silicon substrate. The epitaxial growth has been characterized by means of *in situ* reflection high-energy electron diffraction (RHEED), ultraviolet photoemission spectroscopy, and x-ray photoemission spectroscopy. A strained phase, *s*-FeSi₂, has been clearly identified and shown to be metallic. This phase could be stabilized by the anisotropic elastic field induced by the epitaxy on the silicon (111) face which prevents a solid-state Jahn-Teller effect from distorting the cubic FeSi₂ structure and opening the gap. Also during the growth, dynamical transitions between the different epitaxial phases have been observed at definite thicknesses (typically in the range 10–20 Å): (i) At the temperature of the silicon substrate $T = 350^\circ\text{C}$, strained *s*-FeSi₂ \rightarrow FeSi; (ii) at $T = 400^\circ\text{C}$, strained *s*-FeSi₂ \rightarrow β -FeSi₂. In our work such dynamical transitions are experimentally observed *in situ* during the growth. This shows that the use of a MBE chamber and *in situ* RHEED are very powerful techniques for studying and controlling metallurgical transformations on nanometer scale in real time. We interpret these dynamical transitions as being due to the combination of two effects: a change in the silicon atomic flux coming from the silicon substrate to the surface and the relaxation of the strained phase.

I. INTRODUCTION

Epitaxial growth of Fe-Si alloys by means of molecular beam epitaxy (MBE) on single crystals of silicon appears of interest for many reasons.¹ The growth of an epitaxial film of β -FeSi₂ on silicon would provide us with a direct-gap semiconductor with silicon as a constituent element. Indeed, contrary to similar compounds such as CoSi₂ and NiSi₂, the compound in equilibrium with silicon at low temperature, β -FeSi₂, is not a metal with a cubic structure but a semiconductor with an orthorhombic structure. Also β -FeSi₂ is a rather peculiar semiconductor as its electronic structure is not based on the well known *sp*³ hybridization, as is the case for other common semiconductors (Si, Ge, GaAs, ...), but on a solid-state Jahn-Teller effect² which is simultaneously the cause of a lattice distortion and a band-gap opening at the Fermi level compared with the metallic state of the fluorite structure of CoSi₂ and NiSi₂.

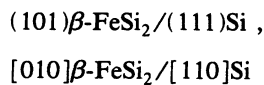
Furthermore, the growth on silicon of a stoichiometric alloy such as β -FeSi₂ introduces the constraint of epitaxial growth together with that of a fixed chemical composition of this alloy. Indeed, contrary to systems with very limited intermixing (such as Ag-Si), the growth of the Fe-Si compounds couples epitaxy and alloying effects since this system presents a large negative enthalpy of mixing. In principle MBE is a very efficient tool to study this problem as it usually provides the number of atoms precisely needed for the growth. Therefore the chemical composition is controlled by the incoming fluxes. A well-known example, GaAs, which has been studied for many years, has shown that almost exactly stoichiometric

materials have been epitaxially grown with a very high quality. Also in that case, symmetrical exchanges between the surface and the vapor phase are possible due to the high vapor pressure of gallium and arsenic at the growth temperature. Together with well-controlled evaporation cells, this allows precise control of the chemical composition at the surface. In the case of iron and silicon, however, it is hardly possible to use evaporation cells due to the low vapor pressure of both elements and to their high chemical reactivity with many crucibles (only alumina crucibles appeared reasonable to us for iron evaporation as long as the temperature is kept below the melting point). Consequently, most of the time electron guns are used for both elements. Despite great achievements in the MBE growths of silicides^{3–5} and even of superlattices,^{4,5} it remains very difficult to control fluxes using electron guns within a precision better than a few percent. Since stoichiometric deviations have been shown to be experimentally important to control the properties of the bulk silicides, this uncertainty is far too large.⁶ Another route which can be investigated to grow stoichiometric silicides like β -FeSi₂ is the chemical beam epitaxy (CBE), in which reactive gases are used. Such a growth technique allows symmetrical exchanges between the substrate and the vapor phase. In principle CBE could open a way to control surface stoichiometry without exchange of atoms with the silicon substrate.

However, up to now the most widely used route to fix the chemical composition and permit epitaxial growth is simply to activate by post-growth thermal annealing the diffusion in between the grown thin film and the silicon substrate.⁷ This is called solid-phase epitaxy (SPE) and it requires a huge atomic diffusion on a long scale that has

been experimentally shown to limit the growth of thick epitaxial films (in the case of β -FeSi₂ prepared by complete annealing of an iron film deposited at room temperature on silicon, 300 Å seems to be the limit for the SPE growth) and to induce the formation of a high density of large holes in the film.⁸ Thus, despite some clear experimental features, a detailed understanding of the SPE growth of silicide alloys does not exist. This understanding is especially hindered as it can involve *transient metastable phases* and *nonequilibrium states*.

In this paper our aim is to present a systematic investigation of the growth of Fe-Si compounds on the silicon (111) face using reactive deposition epitaxy (RDE). The basic experimental conditions for each growth were (i) a fixed-flux atomic beam of iron sent to the surface and (ii) a constant temperature of the substrate during the growth. For all experiments performed, the temperature was varied from 50 °C up to 600 °C in order to control the silicon diffusion toward the surface. As schematically presented in Fig. 1, depending upon the temperature of the substrate, an effective flux of silicon diffuses through the growing film. This silicon flux is basically controlled by the temperature of the substrate and by the thickness of the film formed. Furthermore, it likely depends also on the chemical nature of the growing film. During the growth an *in situ* real-time RHEED pattern acquisition was performed. Each epitaxial phase appearing at the surface can then be identified to determine its epitaxial relationships with silicon. As it appears in the equilibrium phase diagram (Fig. 2), the silicide in equilibrium with silicon is β -FeSi₂. Indeed, at high temperature where interdiffusion is very active, β -FeSi₂ forms readily. At $T \approx 550$ °C, the epitaxial growth of β -FeSi₂ is definitely observed. This will be part of the results presented in this paper. In this case of β -FeSi₂ on the silicon (111) face, the epitaxial relationships as checked by RHEED, LEED, and electron microscopy are¹



or, as β -FeSi₂ presents an orthorhombic structure with only a small difference between the *b* and the *c* axis ($b = 7.83$ Å, $c = 7.79$ Å):

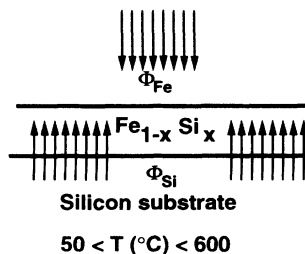
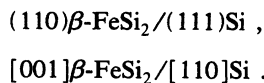


FIG. 1. Schematic presentation of a RDE experiment. The key parameters are indicated: the temperature of the substrate and the iron flux. The effective silicon flux depends on all these parameters and on the thickness of the film.

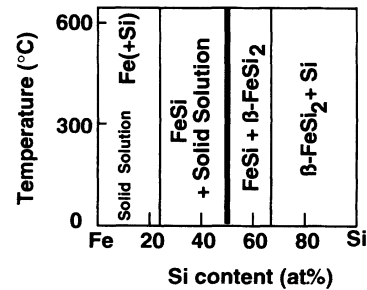
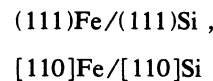


FIG. 2. Low-temperature part ($T < 600$ °C) of the iron-silicon equilibrium phase diagram.

The reciprocal lattice of the β -FeSi₂ epitaxial face is presented in Fig. 3. Since this β -FeSi₂ epitaxial face has a rectangular symmetry and the (111) silicon face a hexagonal one, three equivalent orientations exist. This is why Fig. 3 exhibits an apparent sixfold symmetry. UPS measurements performed on the grown β -FeSi₂ film will be shown to be consistent with the existence of a forbidden gap ($E_g \sim 0.9$ eV). On the contrary, if the temperature is kept close to the room temperature, the interdiffusion is completely frozen out and deposition of iron on silicon should result in the growth of an iron film on silicon. This is actually what has been repeatedly observed since epitaxial relationships of iron on silicon have been independently measured by different groups:⁹



This coexistence of iron and silicon is a nonequilibrium state. In the intermediate temperature range ($T \approx 350$ °C) we shall show that the growth of an epitaxial thin film of FeSi is clearly identified. The RHEED diffraction pat-

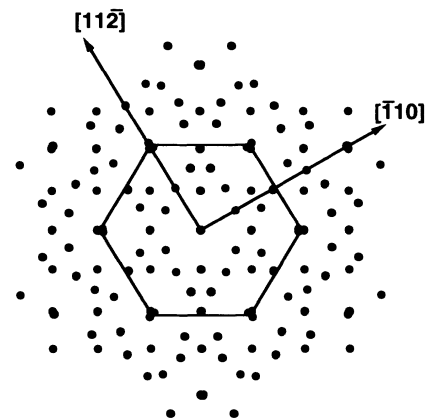


FIG. 3. Two-dimensional reciprocal lattice of the (101) β -FeSi₂ face epitaxially matched on the (111) silicon face. The noticeable sixfold symmetry is due to the existence of three equivalent orientations of the (101) β -FeSi₂ face on the silicon (111) face. The solid lines present the 1×1 reciprocal cell of silicon (111) face.

terns exhibit a $(\sqrt{3} \times \sqrt{3})R 30^\circ$ surface structure. FeSi is a simple cubic structure with a lattice parameter of $a = 4.4 \text{ \AA}$. The epitaxial relationships for this compound are¹⁰

$$(111)\text{FeSi}/(111)\text{Si} ,$$

$$[112]\text{FeSi}/[110]\text{Si} .$$

The reciprocal lattice of the FeSi (111) face is presented in Fig. 4. UPS measurements performed on this grown film will show that FeSi exhibits a strong metallic character.

Therefore, reactive deposition epitaxy enabled us to grow epitaxially any low-temperature phase of the Fe-Si phase diagram depending essentially upon the temperature of the silicon substrate. Also we shall see that in the temperature range ($T \approx 350\text{--}450^\circ\text{C}$) a strained $s\text{-FeSi}_2$ epitaxial phase grows on silicon for very small thicknesses ($< 20 \text{ \AA}$). It does not exist in the equilibrium phase diagram and it is stabilized by the epitaxial growth on the silicon (111) face. RHEED patterns of this phase will be shown to present a 2×2 surface structure [Fig. 5(a)]. The comparison of Figs. 5(a) and 5(b) shows that it is possible to distinguish between the structure of these two FeSi₂ phases. In a RHEED experiment, if the electron beam is aligned along a $[112]$ azimuth of silicon, the existence of a diffraction streak at $1/4$ of the 1×1 silicon diffraction streak is evidence of the $\beta\text{-FeSi}_2$ structure. If no other streaks than those associated with the 2×2 diffraction patterns are observed, we can conclude that only the strained $s\text{-FeSi}_2$ is growing. Also, the way we have determined that this strained phase presents a chemical composition FeSi₂ will be described. In a following section of this article, we shall show how this strained phase is stabilized during deposition of iron on a heated silicon surface. The study of electronic properties by means of UPS will show that this phase presents a metallic character.¹¹ Recently the existence of a strained FeSi₂ phase prepared directly by codeposition of Fe and Si at low temperature was independently reported.¹² This phase presents a cubic structure and is metallic. Further experimental results are needed to quantitatively compare these two strained FeSi₂ phases, which are likely to be close even though they have been prepared in two

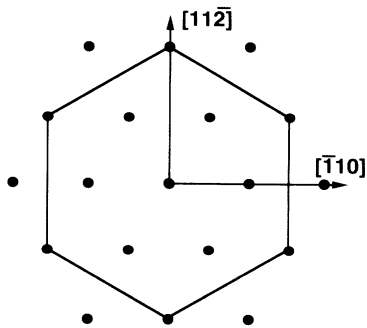


FIG. 4. Two-dimensional reciprocal lattice of the (111) face of FeSi. The hexagon shows the reciprocal lattice of the (111) face of silicon (solid line).

different ways. In any case, they reveal a unique effect, as this means that the semiconducting state and the lattice distortion induced by the Jahn Teller effect are suppressed by the epitaxy on the silicon (111) face and that the strained FeSi₂ compound is probably stabilized in the fluorite structure of NiSi₂ and CoSi₂. The temperature range in which this strained phase is observed, together with the measured critical thicknesses, are presented in this paper. Also, the interplay between all these different phases during the epitaxial growth will be shown. Indeed, coming from the low-temperature regime with the coexistence of an iron film and the silicon substrate to the high-temperature one where $\beta\text{-FeSi}_2$ is growing readily, there are only limited possibilities for the system to accommodate large changes in the thermally activated silicon flux outdiffusing from the substrate to the surface. Therefore, at a fixed temperature, transitions between the different Fe-Si compounds are expected as the growth proceeds and the surface becomes increasingly further away from the original silicon surface. We shall show in the present paper that these transitions are indeed observed. It is remarkable to see that epitaxial growth is maintained through these transitions even though they imply dramatic chemical changes.

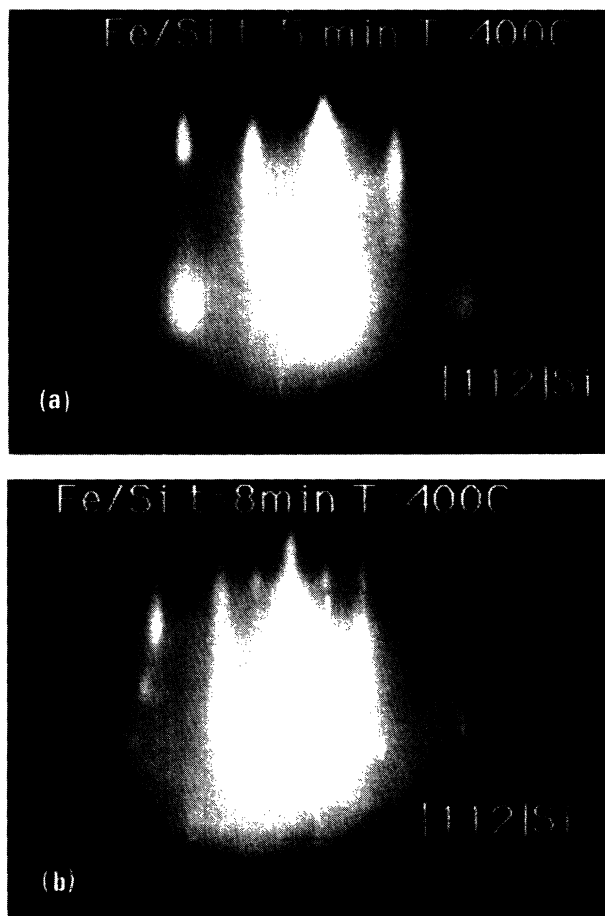


FIG. 5. RHEED patterns along the $[112]$ silicon azimuth during iron deposition on a silicon substrate at $T = 400^\circ\text{C}$: (a) the initial 2×2 surface structure; (b) the surface structure characteristic of the relaxed $\beta\text{-FeSi}_2$ phase.

II. EXPERIMENT

Growth of iron on (111) oriented silicon wafers (2 in. diameter) was performed in a MBE machine equipped with silicon and iron evaporation cells. The base pressure of the MBE chamber at room temperature was between 1×10^{-10} and 2×10^{-10} Torr. The silicon source with a small flux (less than 1 Å/min.) was used to clean the silicon surface. During the growth, the iron flux we have used was about 1 Å/min. Cleaning of the silicon was based on two stages: (i) an *ex situ* chemical etching following the classical Shiraki procedure and (ii) a desorption of the native oxide by heating the wafer at 800 °C associated with an atomic beam of silicon on the surface. Such a treatment resulted in a reproducible, well-defined 7×7 reconstructed silicon surface.

Results presented here mainly come from *in situ* RHEED and electron spectroscopy experiments, our MBE apparatus being equipped with a 10-keV electron gun and connected to a multitechnique analysis chamber with UPS and XPS facilities. For RHEED experiments, the grazing angle of the electron beam with the surface was about 1°. A camera periodically took pictures of the RHEED patterns (the acquisition period could be changed from 10 pictures/sec up to 1 picture/day) which were stored in a computer. Image analysis was then performed. Intensities of diffraction spots were extracted from the RHEED pattern. The temperature control was better than 1 °C for both the substrate and the evaporation cells as measured on their respective thermocouples. The accuracy of the temperature measurement was controlled on the crystallization of amorphous silicon and on the $7 \times 7 \leftrightarrow 1 \times 1$ transition at the silicon surface: the temperature shift should not be larger than 10–20 °C. After the epitaxial growth in the MBE chamber, samples were transferred in the analysis chamber. During sample transfer, the vacuum was about 10^{-9} Torr. UPS and XPS measurements were performed using the helium radiation at 21.2 eV (He I) and the aluminum $K\alpha$ radiation of 1486.6 eV, respectively. Spectra have been recorded for both UPS and XPS using a hemispherical V.S.W. analyzer with a diameter of 150 mm. During the UPS measurements, the base pressure in the analysis chamber was 3×10^{-8} Torr of helium. With the experimental set-up used during the UPS experiments, the energy resolution has been determined by measuring the energy width of the decrease of the electronic density of states at the Fermi level of a clean silver foil. This width was about 100 meV. This gives the minimum energy width of meaningful details in UPS spectra. We have used XPS to determine the chemical composition at the surface and UPS to characterize the electronic properties of the grown film.

III. RESULTS

Using diffusion coefficients of Fe in silicon and of Si in iron, it is possible to roughly estimate the silicon substrate temperatures needed for significant silicon-iron interdiffusion. This does not enable us to describe quantitatively our experiments because data on nucleation of

different phases are not included in these calculations. Table I contains diffusion coefficients taken from Ref. 14. In Table II, the average distances $(\langle X^2 \rangle)^{1/2}$ traveled in one minute are presented for different temperatures. Even though there are probably important uncertainties in D_0 and E_a for both couples of diffusion, a striking feature is the very high diffusivity of iron in silicon. That an iron film of very small thickness can be stabilized on a silicon surface is likely due to the fact that iron solubility in silicon is about zero, as can be seen in the equilibrium phase diagram (Fig. 2). For the reciprocal couple, Si in iron, the solubility is rather high but temperatures as high as 250–300 °C are needed in order to activate the diffusion on an atomic scale (larger than 1 Å) during the characteristic times of measurement. We have experimentally seen surface changes in this range of temperature during annealing of epitaxial iron films deposited on silicon.^{8,10} Using Ref. 14 data, it has been possible to show numerically that these important surface changes observed by RHEED at about 300 °C during annealing of iron films can be analyzed as the sudden arrival of silicon atoms at the surface. Indeed this has been studied by Auger profilometry on a set of thick films (a few thousand angstroms) annealed at temperatures characteristic of surface changes.¹⁵ As expected from Ref. 16, the different phases of the phase diagram are successively formed during thermal annealing. For an epitaxial film of iron (around 1000 Å) on an infinite crystal of silicon (the actual thickness of the silicon crystal is about 300 μm), as the diffusion is started, polycrystalline FeSi is first formed throughout the whole film at 380 °C, and as the temperature is continuously increased, the formation of polycrystalline FeSi₂ follows. Our results are therefore consistent with the diffusion coefficient given in Ref. 14. Since we have experimentally observed the first signs of intermixing in the temperature range of 200–300 °C where the diffusion of silicon in iron becomes active, we conclude that the diffusion of silicon in iron is the relevant one to trigger the first stages of intermixing (However, this does not mean that it remains so once a compound is formed at the interface. More experimental work is needed to definitely identify the efficient diffusion mechanisms during a complete intermixing). For deposition of iron on silicon at different substrate temperatures, this fixes the temperature range to be used. So we have sent an atomic flux of iron on the silicon (111) surface at the following temperatures: 50, 300, 350, 400, 450, and 550 °C.

A. Substrate temperature $T \approx 50-80$ °C MBE growth of iron on silicon

The characteristic features of the iron epitaxial growth at temperatures slightly above room temperature (around

TABLE I. Activation energy E_a and diffusion coefficient D_0 of thermal diffusion for iron atoms in silicon and for silicon atoms in iron.

	Fe-Si	Si-Fe
E_a (kJ/mole)	84	200
D_0 (Cm ² /s)	0.0062	0.7

TABLE II. Distances traveled by a silicon atom in iron and by an iron atom in silicon in one minute for different characteristic temperatures.

T (K)	$(\langle X^2 \rangle)^{1/2}$	$(\langle X^2 \rangle)^{1/2}$
	(Å)	(Å)
	Si-Fe	Fe-Si
300 (RT)	10^{-8}	3
500 (230 °C)	10^{-2}	2500
600 (330 °C)	1.3	

50–80 °C) on silicon (111) have been published in Ref. 9. The grown film is chemically pure iron film as measured by Auger profilometry. The thickest epitaxial iron film we have grown was about 2500 Å thick. This is probably not the limit for the epitaxial growth of iron on silicon.

B. Substrate temperature $T \approx 300$ – 350 °C

As the temperature is increased, thermal diffusion of silicon is activated. During deposition of iron on the silicon (111) face at temperatures between 300 and 350 °C, RHEED patterns recorded as the growth proceeded display completely different features: at the beginning of the iron deposition until the equivalent thickness of a pure iron film of about 5 Å, the epitaxial growth of iron was no longer observed, but instead a 2×2 surface structure was seen. Such a surface structure is shown in Fig. 6 (a). At the precision of RHEED, the lattice parameter of this structure measured parallel to the surface is equal to the one of silicon: it is a strained thin film. Furthermore, the RHEED streaks observed on the electron diffraction pattern [Fig. 6(a)] exhibit remarkable features. Streaks which are at the location of 1×1 silicon diffraction streaks display localized spots at positions which form on the whole screen, a rectangular lattice. Along the [112] azimuth of silicon, this can be analyzed as the electron diffraction of a rough surface of a cubic crystal. Analysis of the RHEED pattern on the [110] azimuth leads to the same conclusion. Half-order streaks do not present well-defined localized spots; so they may be due to flat parts of the surface. The diffracting object which gives rise to these half-order streaks should not have an extension perpendicular to the surface, otherwise, as on 1×1 streaks, localized spots would be seen. Therefore the RHEED streaks on this phase are consistent with a cubic phase and a 2×2 surface reconstruction. One can notice that this result has been repeatedly reported for silicides with a fluorite structure such as CoSi_2 .^{3–5} A strained cubic phase with a similar surface reconstruction has recently been inferred for FeSi_2 by scanning tunneling microscopy measurements.¹⁷ However, taking into account only the phases described in the Fe-Si equilibrium phase diagram, no clear analysis has been found to describe this phase and its epitaxial relationships with silicon.¹⁸ XPS and UPS measurements have been performed on this phase. The ratio measured by XPS between Fe 3*p* and Si 2*p* peaks is quite close to what has been measured for β - FeSi_2 . As can be seen in Fig. 7, the measured UPS spectrum clearly exhibits an important peak at energies just below the Fermi level (at about 1.5 eV below it). This is

expected for a Fe-Si compound with an important *d*-band character due to iron atoms. A more detailed analysis shows that the spectrum does not present a tail of low electronic density of states at the Fermi level characteristic of a semiconductor, but instead a shoulder which crosses the Fermi level. This is an indication that available occupied electronic states are located at the Fermi level and therefore that this phase presents a metallic character. As the film thickness increased beyond 5 Å equivalent iron, an important and gradual structural change is observed by RHEED. Figures 6(b) and 6(c) shows this change. At this stage of the growth, the 2×2 diffraction pattern gradually disappeared and instead the characteristic diffraction patterns ($\sqrt{3} \times \sqrt{3}$) R 30° surface structure emerged [Figure 6(d)]. This is an irreversible transformation from the growth of the strained phase characterized by a 2×2 surface structure to the growth of the FeSi compound characterized by the ($\sqrt{3} \times \sqrt{3}$) R 30° pattern. This transition is quantitatively described in Fig. 8. During the growth, no experimental parameters we can control were changed. Therefore such a transformation is a dynamical change occurring during the growth.

UPS measurements performed on this FeSi phase (Fig. 9) are quite different from the results obtained on the previous phase and they present the characteristic shape of FeSi as it is reported in Ref. 19. In some references, FeSi is reported to have a narrow forbidden gap (≈ 0.05 eV) at the Fermi level. If this gap exists, it cannot be determined with the resolution of our spectrometer (≈ 0.1 eV). In our measurements, FeSi is found to have a strong metallic character. At larger film thicknesses (about 100 Å equivalent iron at $T \approx 350$ °C), a new change was observed. Diffraction rings in RHEED were observed from the surface, which means that disoriented crystals are growing on the surface. Finally no evidence for epitaxial growth was left on the screen.

C. Substrate temperature $T \approx 400$ – 450 °C

At higher temperatures, between 400 and 450 °C, a new regime was observed. Still at the beginning of the growth, RHEED patterns were again characteristic of the 2×2 surface structure. Again during the growth, a gradual change occurred in the same range of thicknesses. But the new phase that appeared was no longer an epitaxial FeSi phase but instead the β - FeSi_2 phase, the compound that is normally in equilibrium with silicon. This epitaxial β - FeSi_2 is well identified. It exhibits its usual epitaxial plane on the silicon (111) face with the three domains since the epitaxial plane of β - FeSi_2 has a rectangular symmetry compared to the hexagonal symmetry of silicon.^{1,2} In Fig. 5, for the [112] azimuth of silicon, the RHEED patterns before and after transformation are shown. The $1/4$ diffraction streak observed in Fig. 5(b) is the signature of the transformation of the strained phase into the relaxed β - FeSi_2 . Quantitative analysis can be performed by measuring the RHEED intensity of the $1/4$ peak. It is presented in Fig. 10. XPS performed on this well-characterized β - FeSi_2 phase shows characteristic peaks such as Si 2*p* and Fe 3*p*. Their inten-

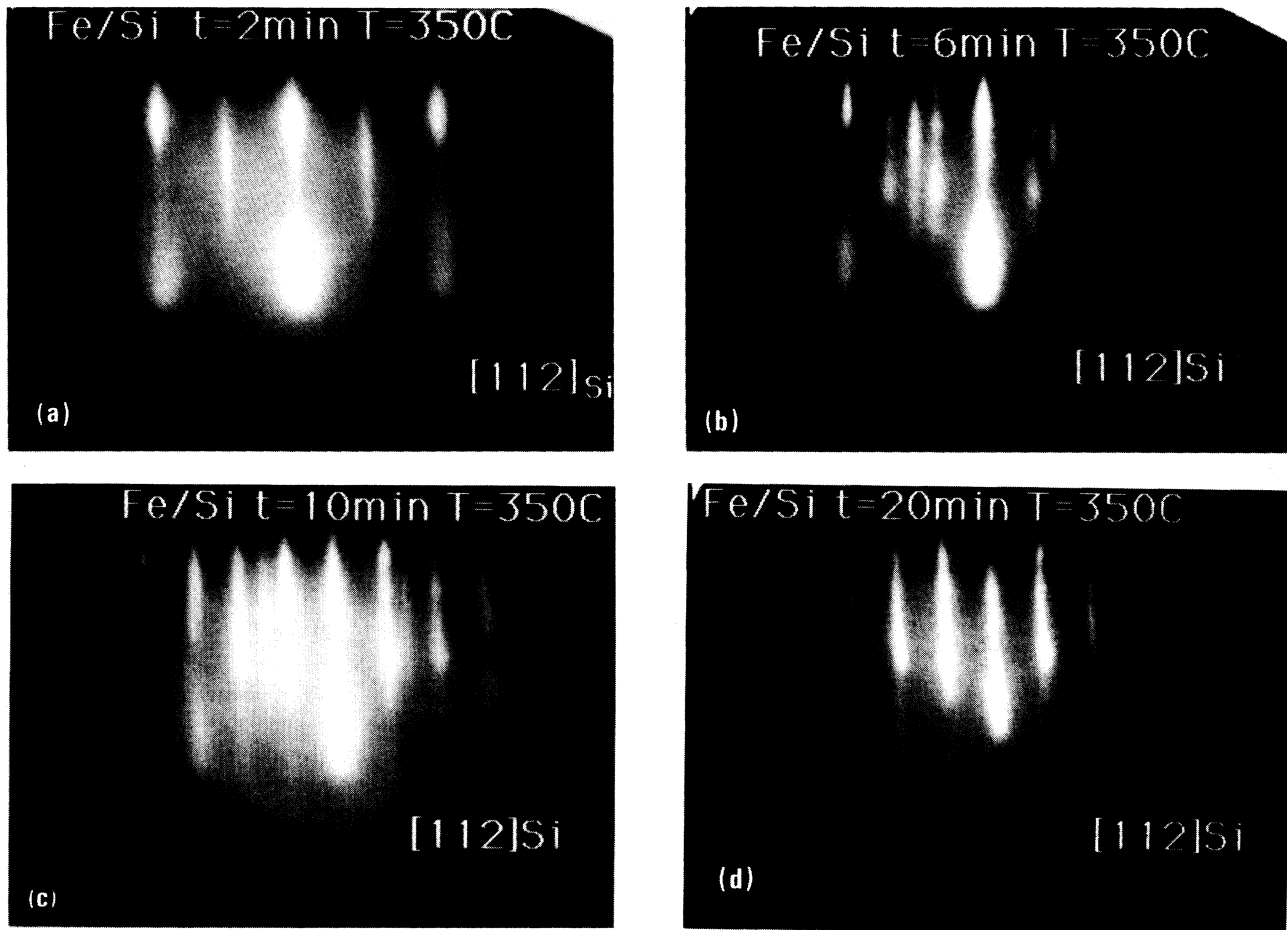


FIG. 6. RHEED patterns along the $[112]$ silicon azimuth during iron deposition on a silicon substrate at $T = 350^\circ\text{C}$: (a) the initial 2×2 surface structure, the transition between the 2×2 surface structure and the $(\sqrt{3} \times \sqrt{3})R30^\circ$ surface structure; (b) after 6 min; (c) after 10 min; (d) the $(\sqrt{3} \times \sqrt{3})R30^\circ$ surface structure.

sities have been used as references to characterize the chemical composition of the strained phase which is measured to be very close to FeSi_2 . An UPS spectrum on this $\beta\text{-FeSi}_2$ is presented in Fig. 11. Our measurements on this phase are consistent with already published results.^{1,13} At lower energy than the Fermi level (about 1 eV below), as in other Fe-Si compounds, the strong d band character is present. At the Fermi level, the curve presents a very low intensity which is the tail of a decreasing signal. Taking into account the energy resolu-

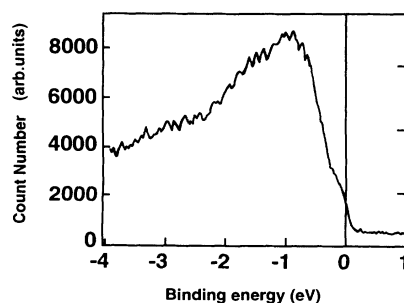


FIG. 7. UPS spectrum measured on a thin film of the FeSi_2 strained phase.

tion of our spectrometer, this result indicates that $\beta\text{-FeSi}_2$ presents a semiconducting character. It should be emphasized that the measured signals for $\beta\text{-FeSi}_2$ and for the strained FeSi_2 phase are clearly different even though the chemical compositions of both phases are experimentally very similar.

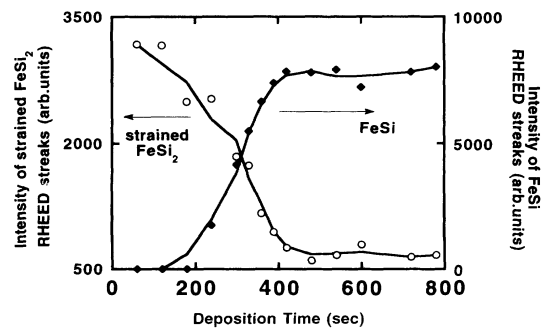


FIG. 8. Plot of intensities of characteristic RHEED peaks of the $s\text{-FeSi}_2$ phase (half-order peak) and of the FeSi phase (peak located at $1/3$ in the RHEED pattern).

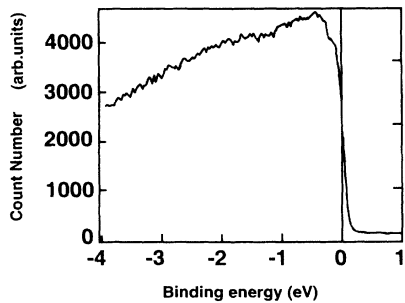


FIG. 9. UPS spectrum measured on a thin film of the FeSi phase.

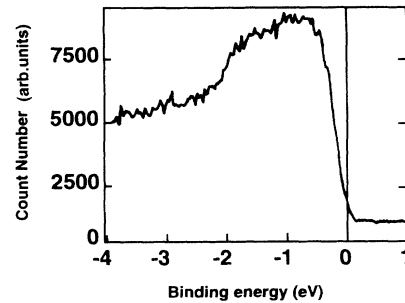


FIG. 11. UPS spectrum measured on a thin film of the β -FeSi₂ phase.

D. Substrate temperature $T \approx 550^\circ\text{C}$

At even higher temperature, from the very beginning of iron deposition, as soon as the 7×7 reconstruction was lost, the epitaxial growth of β -FeSi₂ was observed with no change toward another epitaxial phase. The only evolution of the RHEED pattern was the gradual disappearance of the diffraction pattern probably due to a decrease in the crystalline quality of the growing film. Indeed a study of the surface after the growth by means of scanning electron microscopy reveals a very rough surface with a high density of large holes (characteristic diameter $\approx 1000 \text{ \AA}$). This emphasizes the fact that even when β -FeSi₂ is immediately formed, only limited thicknesses of β -FeSi₂ are prepared epitaxially on silicon and thus with a rough surface containing large holes.

The experimental results we have presented in this section are summarized in Fig. 12. To interpret such an effective phase diagram, two experimental parameters have to be taken into account. First the RHEED technique is a highly surface-sensitive technique. This means that we have limited information on the final structure of the grown film. It remains to determine if the structure of the film is homogeneous despite the surface changes in the epitaxial growth or if it is a *layered* structure. Also, Fig. 12 could be quantitatively dependent upon the iron flux coming on the surface. The dependence of the ob-

served phase transformations as the iron flux is changing remains to be investigated.

IV. CONCLUSION AND DISCUSSION

Figure 12 shows that at least four different states are observed during the epitaxial growth. Two key points call for comments: (i) a strained FeSi₂ phase has been observed which can relax toward β -FeSi₂; (ii) dynamical transformations between phases have been observed during the growth.

For the first point, diffraction experiments at the surface on an unknown phase do not allow a direct determination of the chemical composition. They have been complemented here by the XPS measurements, which show that the strained phase has a composition very close to FeSi₂. However, the chemical composition can also be deduced from the growth behavior. This strained phase grows at a temperature where the silicon thermal diffusion is sufficiently activated to ensure the growth of β -FeSi₂ as soon as relaxation take place (see the experiment at 400°C in Fig. 5). So this is a strong indication that, in this temperature range, the chemical composition

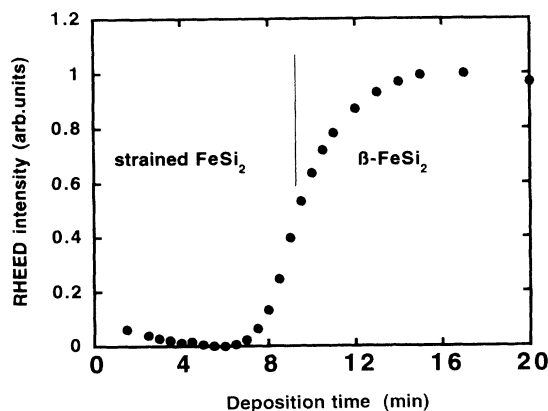


FIG. 10. Plot of the intensity of the 1/4 peak characteristic of β -FeSi₂ versus the deposition time. The critical thickness can be directly determined: $e_c(\beta\text{-FeSi}_2) \approx 30\text{--}40 \text{ \AA}$.

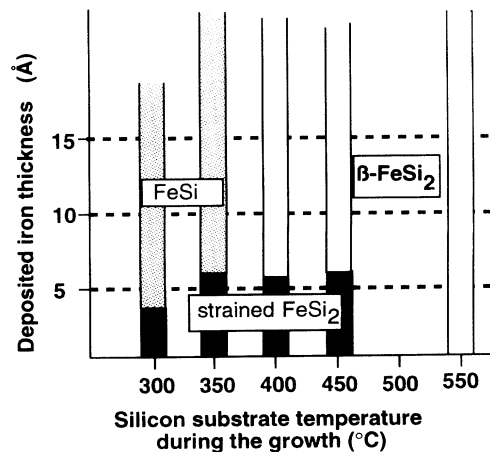


FIG. 12. Phase diagram describing RDE growth of iron silicides.

of the strained phase is locked at FeSi_2 , the chemical composition in equilibrium with silicon. Although not precisely identified as a strained FeSi_2 phase at the time of the experiment, one can find in Ref. 20 experimental evidence for the same strained phase stabilized by solid-state interdiffusion. Auger spectroscopy on this phase has shown that the composition is indeed very close to FeSi_2 . It exhibits an hexagonal symmetry as indicated by low-energy electron diffraction within the epitaxial plane and a 2×2 surface reconstruction. The surface diffraction would then be very much consistent with a cubic phase displaying a 2×2 surface reconstruction. It is likely that this phase is close to a strained fluorite phase having within the plane of epitaxy the lattice parameter of silicon at the precision of RHEED.¹⁸ The structure of the beta phase supports this interpretation as its semiconducting state arises from a Jahn-Teller effect^{2,10} for which evidence is simultaneously found in the opened gap of the $\beta\text{-FeSi}_2$ electronic structure and in an important distortion of the fluorite structure which lowers the crystalline symmetry from cubic to orthorhombic.²¹ If the fluorite structure is the natural metallic phase associated with the $\beta\text{-FeSi}_2$ semiconducting phase, it is then very surprising to find the specific volume of this hypothetical fluorite phase to be larger than that of the actual semiconducting phase.² Contrary to most common semiconductors, this means that a negative pressure should be applied to put $\beta\text{-FeSi}_2$ in a metallic state. This is in fact what could happen because of the epitaxy on the (111) face of silicon at least for very small thicknesses: the surface cells of the (101) $\beta\text{-FeSi}_2$ face and of the (110) face, which are usually found as epitaxial planes, have an edge much shorter (respectively by 5.3% and 5.5%) than the corresponding one on the silicon face. Therefore the uniaxial stress applied by the silicon surface could put a thin FeSi_2 film under substantial tensile stress. This introduces a critical thickness associated with a stress-induced structural phase transformation. Such a structural transformation is associated with an electronic transition since the semiconducting state is very much linked with the orthorhombic structure. Below this critical thickness, FeSi_2 is metallic and, matched with silicon in the plane of epitaxy and above, exhibits its semiconducting relaxed β phase. Very recently other results have appeared which basically agree with this analysis of the strained phase. The cubic structure has been directly observed through transmission electron microscopy and Rutherford backscattering on a strained phase prepared by laser melting of a thin iron disilicide thin film.¹² Observation with the electron beam parallel to the interface gave direct evidence for the cubic symmetry. Also, this technique, contrary to our experiment, has been able to extend the critical thickness up to about 300 Å. The origin of this difference is not definitely clear to us as the two preparation techniques are quite difficult to compare. The metallic state has also been observed together with the transition toward the semiconducting state on thin films grown by MBE.¹³ In conclusion, the effect of the silicon (111) face on the epitaxy of FeSi_2 has been clearly evidenced. We are probably dealing with an electronic and structural phase transition induced by the strain field of silicon during the ep-

itaxial growth. This effect appears rather unique.

The second key point is the induced chemical and structural transformation of the growing phase as the growth proceeds. A comparison of Figs. 5 and 6 directly shows what seems to us a central result presented in this paper. By changing the temperature of the substrate by only 50 °C, completely different behaviors are observed. Starting at both temperatures ($T = 350$ and 400 °C) with the same initial state at low thicknesses, the strained phase of FeSi_2 [it is hardly possible to see a difference between Fig. 5(a) and Fig. 6(a)], two completely different evolutions are clearly identified after further iron deposition. It seems to us that this is an effect particular to reactive deposition epitaxy. In the case of codeposition of both species with no possible chemical exchange with the substrate, such a change in the chemical composition appears quite impossible because the ratio of species is fixed by atomic fluxes. In the case of deposition of iron on a heated silicon substrate, which can be considered as an infinite buffer of silicon atoms, the chemical potential is fixed by the silicon. Therefore the obvious equilibrium state is the coexistence of silicon and iron disilicide. Only kinetic effects can prevent the system from reaching this point. At high temperatures (for the iron flux we used this means $T > 500$ °C as described in Fig. 5) the silicon diffusion is sufficiently activated to ensure the formation of $\beta\text{-FeSi}_2$ (at least in the range of thicknesses we have investigated). At lower temperatures, the silicon diffusion enables the formation of FeSi_2 only at very low thicknesses. Since the temperature is kept constant and the silicon buffer appears increasingly further away from the surface, one could explain our experimental results in the temperature range 300–350 °C by a lack of silicon atoms at the surface. Since a continuous decrease of silicon concentration is not allowed by the equilibrium phase diagram in this range of temperature, the only remaining way for this system is to jump to the next silicide with a lower silicon concentration. This is indeed what we characterize with our results. The loss of epitaxy at slightly higher thickness in fact could be due to a following jump in the phase diagram toward an iron-rich solid solution. The electron surface diffraction in this last regime was not clear enough to experimentally assess this conclusion. The results obtained in the intermediate regime of temperature provide us with clear evidence for a dynamical irreversible transition in between two silicides $\text{FeSi}_2 \rightarrow \text{FeSi}$. To our knowledge such a dynamical transition during deposition on a heated silicon substrate has not been clearly presented before for the growth of other silicides on silicon. That we have found clear evidence only for transitions in which the strained phase is involved could explain why this effect has not been observed for metallic and cubic silicides ($\text{CoSi}_2, \text{NiSi}_2$). Indeed, for these silicides the pseudomorphic growth observed at low thicknesses does not involve a complete change of the crystal structure and an electronic transition. A strained phase with structure and electronic properties different from the equilibrium state does not exist at all for CoSi_2 and NiSi_2 . Strictly looking at the available experimental results on metallic silicides, the existence of such dynamical transitions during growth on a

heated silicon surface remains for us an open question. The influence of relaxation of the FeSi_2 phase on the interface energy at the Si/FeSi_2 interface and on the diffusion of different species at this interface may be an important parameter to be considered in order to understand nucleation of different phases during growth.

Furthermore, many questions have not yet been investigated but are direct consequences of the major results presented in this article. We do not know if thicknesses at which transitions occur are influenced by changes in the iron flux, nor do we know the structure of the whole film after a transition. At $T = 350^\circ\text{C}$, we have no experimental evidence to determine whether FeSi_2 still exists between FeSi and the silicon substrate.

ACKNOWLEDGMENTS

We thank R. Pantel and F. Arnaud d'Avitaya for their help with Auger measurements, and S. Calisti and J. P. Dussaulcy for technical assistance. This work was supported by the European Community through the Esprit Basic Research Action Project No. 3026. Grants from the French Ministère de la Recherche et de la Technologie (Contracts Nos. 88R0973 and 90S0249) and from the PIRMAT-CNRS are also gratefully acknowledged. The Centre de la Recherche sur les Mécanismes de la Croissance Cristalline is a Laboratoire associé aux Universités d'Aix-Marseille II and III and is Laboratoire propre du Centre National de la Recherche Scientifique.

-
- ¹J. Derrien, J. Chevrier, Le Thanh Vinh, and J. Mahan, *Appl. Surf. Sci.* **56/58**, 382 (1992); N. Cherief, C. d'Anterroches, R. Cinti, T. A. Nguyen Tan, and J. Derrien, *Appl. Phys. Lett.* **55**, 1671 (1989).
- ²J. Labbé and J. Friedel, *J. Phys. (Paris)* **27**, 153 (1966); D. Adler and H. Brooks, *Phys. Rev.* **155**, 826 (1967); U. Birkholz and J. Schlem, *Phys. Status Solidi* **27**, 413 (1968); **34**, K177 (1969); N. E. Christensen, *Phys. Rev. B* **42**, 7148 (1990).
- ³J. Derrien and F. Arnaud d'Avitaya, *J. Vac. Sci. Technol. A* **5**, 2111 (1987).
- ⁴H. von Känel, J. Henz, M. Ospelt, and P. Wachter, *Phys. Scr.* **T19**, 158 (1987).
- ⁵R. T. Tung, in *Silicon Molecular Beam Epitaxy*, edited by E. K. Kasper and J. C. Bean (CRC, Boca Raton, FL, 1988), Vol. 2, p. 13.
- ⁶P. Gas (private communication).
- ⁷F. M. d'Heurle, *J. Mater. Res.* **3**, 167 (1988).
- ⁸J. Chevrier, V. Le Thanh, and J. Derrien, *Conference ECO4*, The Hague, 1991, edited by C. Corsi, J. M. Baisceras, and A. J. Kreisler, SPIE Proceedings Series Vol. 1512 (SPIE-The International Society for Optical Engineering, The Hauge, 1991), p. 279.
- ⁹J. Chevrier, V. Le Thanh, R. Buys, and J. Derrien, *Europhys. Lett.* **16**, 737 (1991); T. Kanaji, T. Urano, A. Hiraki, and M. Iwami, in *Proceedings of the Eighth International Vacuum Congress*, Vacuum Congress, Cannes 1980, edited by F. Abélès and M. Croset, Supplement to the journal *Le Vide, Les Couches Minces*, Vol. 201, Tome I (1980), p. 117.
- ¹⁰J. Chevrier, V. Le Thanh, S. Nitsche, and J. Derrien, *Appl. Surf. Sci.* **56/58**, 438 (1992).
- ¹¹We have also identified this strained phase in epitaxial films prepared by deposition of a thin iron film on a cold silicon substrate followed by an annealing (see Ref. 10).
- ¹²M. G. Grimaldi, P. Baeri, C. Spinella, and S. Lagomarsino, *Appl. Phys. Lett.* **60**, 1132 (1992).
- ¹³N. Onda, J. Henz, E. Muller, K. A. Mäder, and H. von Känel, *Appl. Surf. Sci.* **56/58**, 421 (1992).
- ¹⁴Y. Adda and J. Philibert, in *La Diffusion dans les Solides*, edited by F. Perrin, 1966 Bibliothèque des Sciences et Techniques Nucléaires (Presses Universitaires de France, Paris, 1966).
- ¹⁵R. Pantel, Le Thanh Vinh, J. Chevrier, F. Arnaud d'Avitaya, and J. Derrien (unpublished).
- ¹⁶U. Gosele and K. Tu, *J. Appl. Phys.* **66**, 2619 (1989), and references therein.
- ¹⁷A. L. Vasquez de Parga, J. de la Figuera, C. Ocal, and R. Miranda, *Europhys. Lett.* **18**, 595 (1992).
- ¹⁸However, up to now, the only structural information on this strained phase has been provided by electron diffraction. At the moment there is no evidence for the atomic structure of this strained phase coming from an x-ray experiment. This means that it is difficult to make a definite conclusion about the space group of this phase and to ascertain that RHEED half-order streaks are taken as evidence for a surface reconstruction.
- ¹⁹B. Egert and G. Panzner, *Phys. Rev. B* **29**, 2091 (1984); J. Alvarez, J. J. Hinarejos, E. G. Michel, G. R. Castro, and R. Miranda, *ibid.* **45**, 14042 (1992).
- ²⁰N. Cherief, Ph.D thesis, Université Joseph Fourier, Grenoble.
- ²¹Y. Dusausoy, J. Protas, E. Wandji, and B. Roques *Acta Crystallogr. Sect. B* **27**, 1209 (1971).

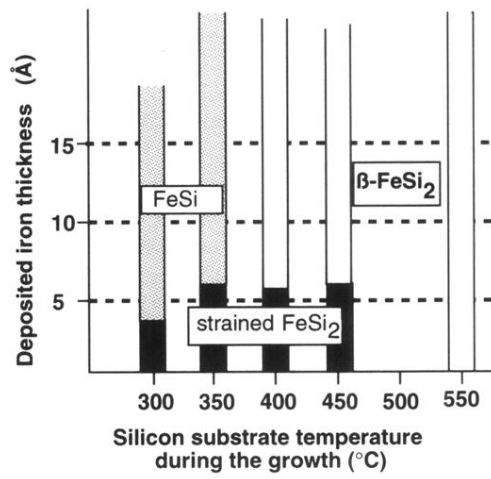


FIG. 12. Phase diagram describing RDE growth of iron silicides.

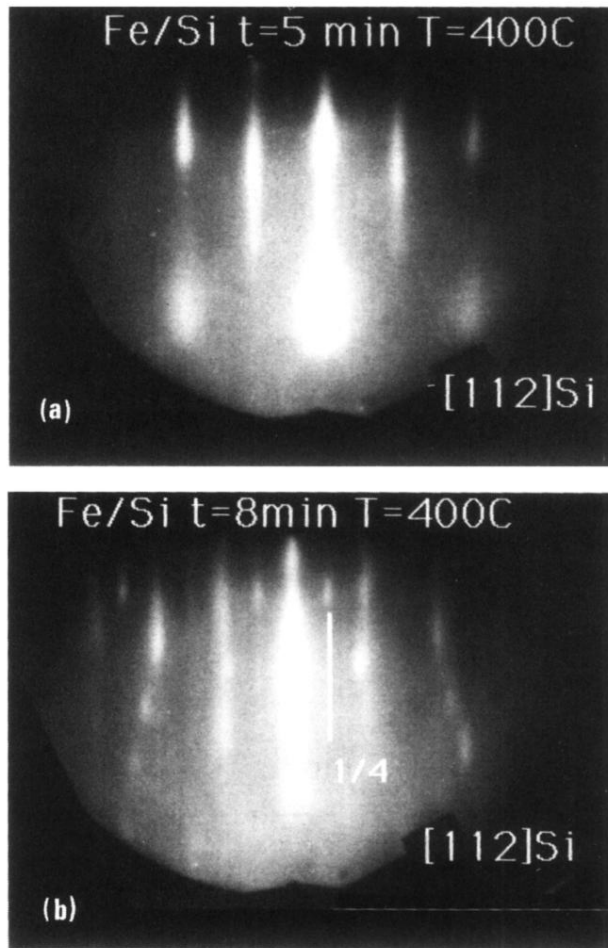


FIG. 5. RHEED patterns along the [112] silicon azimuth during iron deposition on a silicon substrate at $T=400^{\circ}\text{C}$: (a) the initial 2×2 surface structure; (b) the surface structure characteristic of the relaxed $\beta\text{-FeSi}_2$ phase.

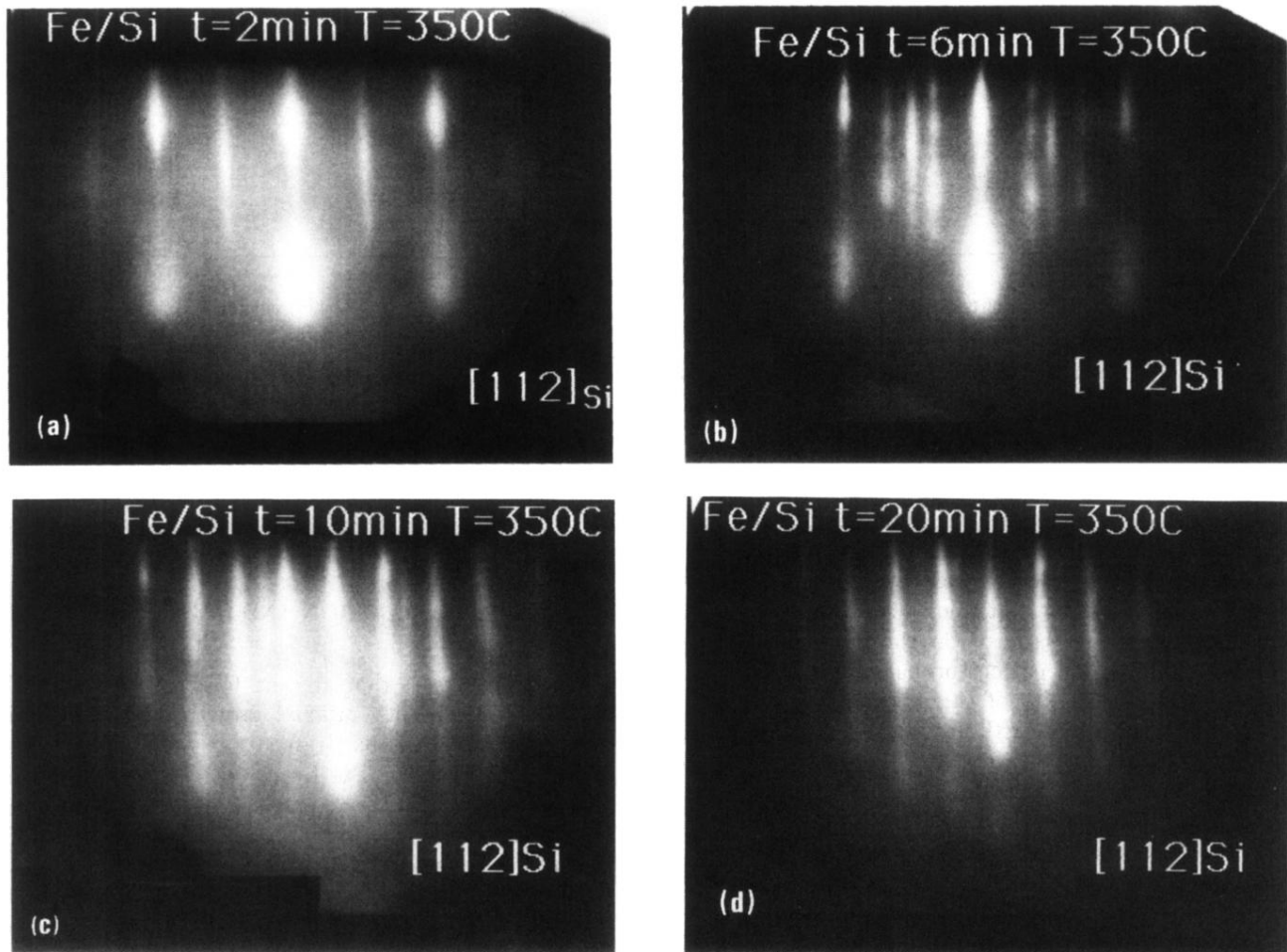


FIG. 6. RHEED patterns along the $[112]$ silicon azimuth during iron deposition on a silicon substrate at $T = 350^\circ\text{C}$: (a) the initial 2×2 surface structure, the transition between the 2×2 surface structure and the $(\sqrt{3} \times \sqrt{3})R 30^\circ$ surface structure; (b) after 6 min; (c) after 10 min; (d) the $(\sqrt{3} \times \sqrt{3})R 30^\circ$ surface structure.